Received: 24 September 2019 | Accepted: 2 December 2019

DOI: 10.1002/mrd.23306

Molecular Reproduction & Development

RESEARCH ARTICLE

Metabolic compounds within the porcine uterine environment are unique to the type of conceptus present during the early stages of blastocyst elongation

Sophie C. Walsh[1] | Jeremy R. Miles[2] | Linxing Yao[3] | Corey D. Broeckling[3] | Lea A. Rempel[2] | Elane C. Wright-Johnson[2] | Angela K. Pannier[1]

[1]Department of Biological Systems Engineering, University of Nebraska-Lincoln, Lincoln, Nebraska

[2]United States Department of Agriculture, U.S. Meat Animal Research Center, Clay Center, Nebraska

[3]Proteomics and Metabolomics Facility, Colorado State University, Fort Collins, Colorado

Correspondence
Jeremy R. Miles, United States Department of Agriculture, U.S. Meat Animal Research Center, Clay Center, NE 68933.
Email: jeremy.miles@usda.gov

Angela K. Pannier, Department of Biological Systems Engineering, University of Nebraska-Lincoln, Lincoln, NE 68583.
Email: apannier2@unl.edu

Funding information
USDA, National Institute of Food and Agriculture, Agriculture and Food Research Initiative Competitive Grant, Grant/Award Number: 2017-67015-26456

Abstract

The objective of this study was to identify metabolites within the porcine uterine milieu during the early stages of blastocyst elongation. At Days 9, 10, or 11 of gestation, reproductive tracts of White cross-bred gilts ($n = 38$) were collected immediately following harvest and flushed with Roswell Park Memorial Institute-1640 medium. Conceptus morphologies were assessed from each pregnancy and corresponding uterine flushings were assigned to one of five treatment groups based on these morphologies: (a) uniform spherical ($n = 8$); (b) heterogeneous spherical and ovoid ($n = 8$); (c) uniform ovoid ($n = 8$); (d) heterogeneous ovoid and tubular ($n = 8$); and (e) uniform tubular ($n = 6$). Uterine flushings from these pregnancies were submitted for nontargeted profiling by gas chromatography–mass spectrometry (GC–MS) and ultra performance liquid chromatography (UPLC)–MS techniques. Unsupervised multivariate principal component analysis (PCA) was performed using pcaMethods and univariate analysis of variance was performed in R with false discovery rate (FDR) adjustment. PCA analysis of the GC–MS and UPLC–MS data identified 153 and 104 metabolites, respectively. After FDR adjustment of the GC–MS and UPLC–MS data, 38 and 59 metabolites, respectively, differed ($p < .05$) in uterine flushings from pregnancies across the five conceptus stages. Some metabolites were greater ($p < .05$) in abundance for uterine flushings containing earlier stage conceptuses (i.e., spherical), such as uric acid, tryptophan, and tyrosine. In contrast, some metabolites were greater ($p < .05$) in abundance for uterine flushings containing later stage conceptuses (i.e., tubular), such as creatinine, serine, and urea. These data illustrate several putative metabolites that change within the uterine milieu during early porcine blastocyst elongation.

KEYWORDS
blastocyst elongation, metabolome, porcine, uterine environment

1 | INTRODUCTION

The preimplantation period of pregnancy in pigs is marked by a rapid transition of the blastocyst in morphology and size. During this period, the blastocyst rapidly transforms from a pre-elongation stage spherical morphology (~1–2 mm) through ovoid (~4–5 mm) and tubular (>10 mm) morphologies, and finally, a filamentous morphology (>100 mm) between days 9–12 of gestation (Bazer, Geisert, Thatcher, & Roberts, 1982; Geisert, Brookbank, Michael Roberts, & Bazer, 1982; Miles, Freking, Blomberg, Vallet, & Zuelke, 2008; Miles, Laughlin, Sargus-Patino, & Pannier, 2017; Pope & First, 1985). Approximately, 20% of embryonic loss occurs due to deficiencies in this process of elongation (Bazer et al., 2009). In order for elongation to be successful, the correct timing and presentation of signaling factors in both the mother and conceptuses are essential. The secretion of factors from the blastocyst and uterus creates the necessary environment in the uterine lumen for elongation to begin and proceed correctly (Bazer et al., 1982; Geisert et al., 2006). At the end of the elongation period, the uterine environment must be ready for superficial implantation of the blastocyst in the uterine endometrium through processes, such as immunosuppression and cellular matrix remodeling (Garlow et al., 2002; Waclawik, 2011).

Improper timing of exposure to signaling factors in the uterine environment has also been shown to create an unfavorable environment for the development of preimplantation conceptuses. Although estrogen exposure within the uterine environment at the final stages of elongation is necessary for the establishment of pregnancy and embryo survival, proper timing of this estrogen exposure is essential. Administration of estradiol valerate to pregnant gilts on Days 9 and 10 of gestation did not prevent blastocyst elongation to filamentous conceptuses on Day 12 of gestation; however, total conceptus loss was evident by Day 16 of gestation (Morgan, Geisert, Zavy, & Fazleabas, 1987). An unfavorable uterine environment deriving from exposure of conceptuses to signaling factors at improper times can also result from diversity of littermate conceptuses, which has been shown to play a role in embryonic and fetal mortality (Bazer, Thatcher, Martinat-Botte, & Terqui, 1988; Pope, Lawyer, Nara, & First, 1986; Pope, Maurer, & Stormshak, 1982). For example, greater synthesis of estradiol from morphologically advanced conceptuses (i.e., filamentous) results in progressed uterine secretions, which creates an unfavorable asynchronous uterine environment for less developed (i.e., ovoid) littermate conceptuses (Wilde, Xie, Day, & Pope, 1988). Additionally, gene regulation, particularly with the transforming growth factor-β family members and steroidogenic pathways, has been demonstrated to be different between homogenous populations of ovoid conceptuses compared with developmental delayed ovoid conceptuses in heterogeneous populations containing advance stage filamentous conceptuses (L. A. Blomberg, Schreier, & Li, 2010). Dramatic differences in the proteomic profiles have been shown within pregnancies of homogeneous populations of ovoid conceptuses compared with homogeneous populations of filamentous conceptuses during the elongation period (Degrelle, Blomberg, Garrett, Li, & Talbot, 2009). Taken together, these findings illustrate the importance of proper timing for presentation and secretion of critical molecular factors in the blastocyst, as well as within the uterine environment on the developmental competence of blastocysts during the preimplantation period of pregnancy. As a result, delays or deficiencies in the initiation of elongation can be detrimental to the survival of pig embryos and can influence within-litter birth weight variability, which plays a key role in piglet mortality.

Although there have been a variety of studies assessing the metabolite content during the porcine reproductive cycle or following in vitro culture of porcine embryos, the metabolome of uterine luminal fluid throughout the initial stages of porcine conceptus elongation has not yet been characterized. For example, Li et al. (2007) analyzed the composition and concentrations of amino acids present in the oviductal and uterine fluids of pigs on Day 3 and Day 5 after estrus to develop a culture medium more closely resembling the uterine environment (Li et al., 2007). A study by Ao et al. (2019) characterized the metabolome of amniotic fluid during pig fetal development and measured corresponding changes in the placental transcriptome to determine associations of changes in these parameters in abnormal development of pig fetuses (Ao et al., 2019). Bertoldo et al. (2013) utilized metabolomics to identify and quantify metabolite composition of follicular fluids from pigs in the follicular phase of estrous, then made correlations of these metabolite characteristics with multiple varying factors including follicular size and the season at collection (Bertoldo et al., 2013). All these studies have demonstrated the importance and utility of metabolomics in the context of porcine reproduction by making advancements in the knowledge of metabolite composition and its changes during porcine reproductive phases allowing for further elucidation of the environment required for successful embryo development and parturition. However, no studies have yet analyzed the metabolite concentrations of uterine fluid in pregnant pigs throughout the early processes of blastocyst elongation, or correlated metabolite concentration changes with specific elongation stage.

It is well known that many maternal- and conceptus-derived factors are present in the uterine lumen during the elongation period of pig blastocyst development. However, many of these factors remain unidentified or uncharacterized, especially when considering interactions between factors or factors that result from cellular processes such as metabolism and growth. The current study aimed to identify metabolites present in the uterine lumen during the initiation and early transitional period of blastocyst elongation and characterize their relative changes at each stage through nontargeted metabolomics profiling to identify novel biomarkers within the uterine milieu that play a role in early blastocyst elongation to better understand the specific factors that contribute to this imperative stage of development.

2 | RESULTS

Uterine flushings were sorted into populations based on the size and morphology of the conceptuses present (Figure 1). Specifically,

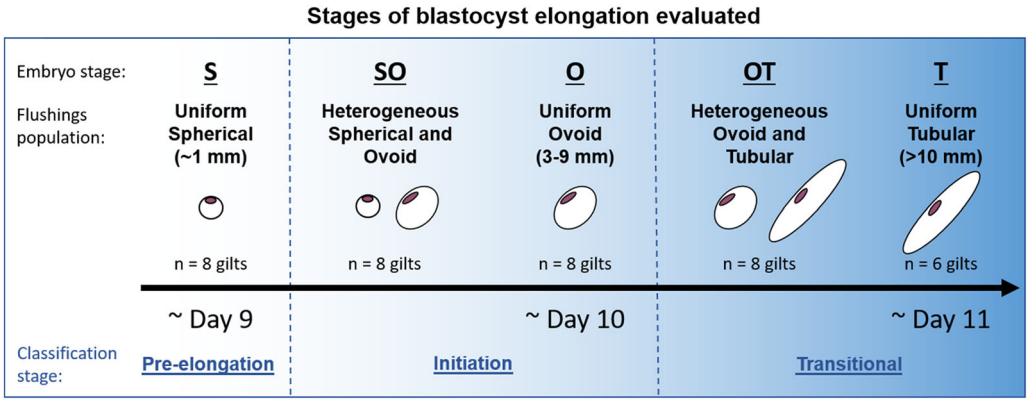

FIGURE 1 To identify metabolites present in the uterine milieu during the early stages of blastocyst elongation, flushings were taken from pregnant gilts on Days 9–11 of gestation. Flushings were sorted into one of five blastocyst treatment groups (flushings populations) according to conceptus morphology (embryo stage): uniform spherical (S, *n* = 8 gilts), heterogeneous spherical and ovoid (SO, *n* = 8 gilts), uniform ovoid (O, *n* = 8 gilts), heterogeneous ovoid and tubular (OT, *n* = 8 gilts), or uniform tubular (T, *n* = 6 gilts). Subsequently, uterine flushings populations were categorized into three classifications of elongation stage (classification stages): (a) pre-elongation stage (S only), (b) initiation stages (SO and O), and (c) transitional stages (OT and T). The average homogeneities for each blastocyst treatment group were: S = 100%; SO = 62%; O = 100%; OT = 56%; and T = 90%

uterine flushings were categorized into five populations: (a) population of uniform spherical stage (S) conceptuses, (b) heterogeneous population of spherical stage and ovoid stage (SO) conceptuses, (c) population of uniform ovoid stage (O) conceptuses, (d) heterogeneous population of ovoid stage and tubular stage (OT) conceptuses, and (e) population of uniform tubular stage (T) conceptuses. These five flushings populations were further categorized into three classifications of elongation based on temporal stage of embryo development: (a) pre-elongation stage, only uniform spherical conceptuses population (i.e., S), (b) initiation stages, heterogeneous population of spherical and ovoid conceptuses, and uniform ovoid conceptuses population (i.e., SO and O), and (c) transitional stages, heterogeneous population of ovoid and tubular conceptus, and uniform tubular conceptuses population (i.e., OT and T). The flushing samples were analyzed using nontargeted metabolomics by both gas chromatography–mass spectrometry (GC–MS) and ultra performance liquid chromatography (UPLC)–MS to produce a more complete metabolic profile. GC–MS analysis detected 153 metabolic features (Table S1) from the flushings, while UPLC–MS analysis detected 103 features (Table S2).

2.1 | Principle component analysis

Principle component analysis (PCA) of both GC–MS and UPLC–MS datasets was performed as a multivariate tool to summarize the metabolome between uterine milieu based on conceptus morphology (Figure 2). These plots illustrate that there are differences in uterine flushings metabolomes corresponding to conceptus morphology. For the GC–MS dataset, the PCA that best described dataset-wide variance was PC1 ($p < .05$) and PC2 ($p < .05$), which collectively explain 54% of the Pareto-scaled dataset-wide variance (Figure 2a). The loading plot for the GC–MS dataset (Figure 2b) demonstrates the weight each individual metabolite contributes to the separation of population samples on the PCA scores plot. This loading plot suggests that uric acid drives the metabolome of uterine flushings containing S conceptuses toward the bottom of the scores plot and phosphoric acid drives the uterine flushings containing S and SO conceptuses to the bottom left. In contrast, serine drives metabolomes toward the top right, separating the uterine flushings of OT and T conceptuses from the other elongation stages. For the UPLC–MS dataset, the PCA that best described the Pareto-scaled dataset-wide variance was PC1 ($p < .05$) and PC3 ($p < .05$), collectively explaining 54% of the variance (Figure 2c). This loading plot (Figure 2d) shows tryptophan as the metabolite that separates the metabolome of uterine flushings containing S conceptuses on the left from the other flushings containing other elongation stage conceptuses (i.e., SO, O, OT, and T). Thus, the results of the PCA suggest that a difference in abundance of uric acid, phosphoric acid, and tryptophan in the uterine flushings of pre-elongation and early initiation stage conceptuses (i.e., S and SO) separate these stages from flushings containing the later transitional stage conceptuses (i.e., OT and T), which alternatively contain differing levels of serine.

2.2 | One-way analysis of variance

Once PCA identified metabolites contributing to the differences in elongation stage metabolomes of uterine flushings, one-way analysis of variance (ANOVA) tests with subsequent Benjamini–Hochburg false discovery rate correction was applied to each of the 153 and 103 compounds detected by GC–MS and UPLC–MS methods, respectively. The results identified 37 GC–MS compounds and 59 UPLC–MS compounds that significantly differed ($p < .05$) within uterine milieu due to the effect of conceptus morphology, illustrated

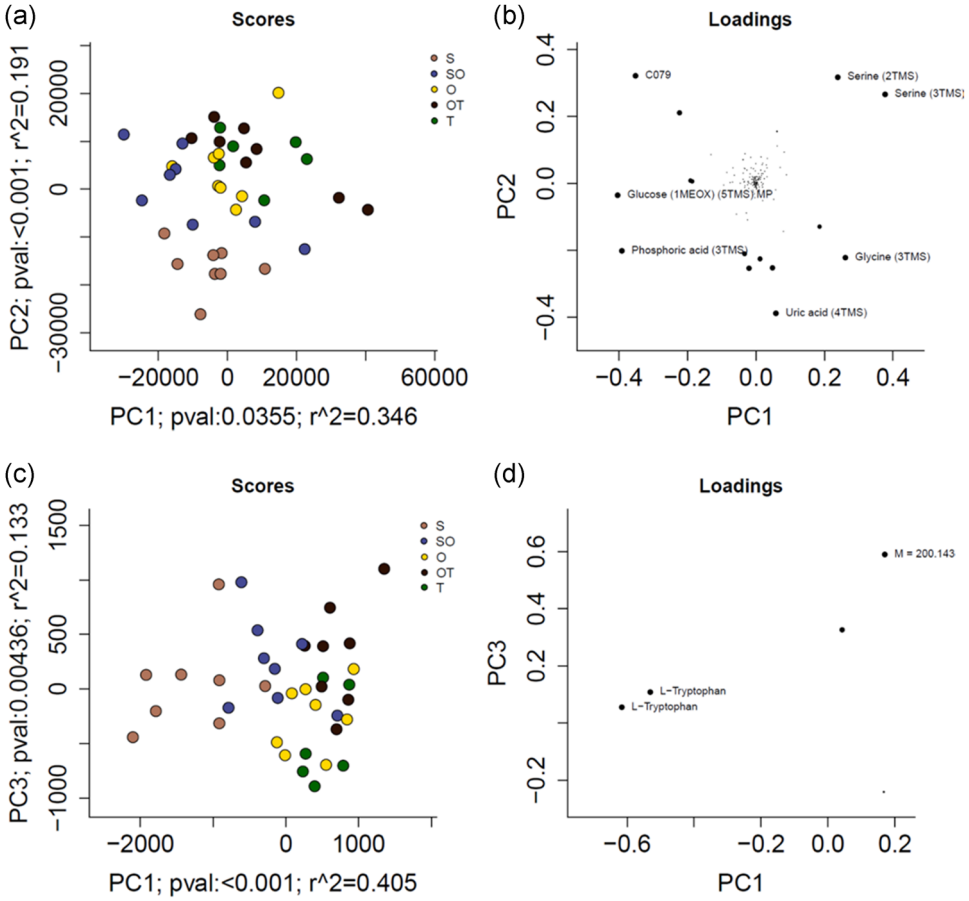

FIGURE 2 Principle component analysis (PCA) scores and loading plots (a/c and b/d, respectively); GC–MS and UPLC–MS datasets (a/b and c/d, respectively). (a) PCA scores plot for the GC–MS dataset illustrates the best separation of uterine milieu based on conceptus morphology resulted from the analysis of PC1 and PC2, which collectively explain 54% of the Pareto-scaled dataset-wide variance. (c) PCA scores plot for the UPLC–MS dataset illustrates the best separation of uterine milieu based on conceptus morphology resulted from the analysis of PC1 and PC3, which collectively explain 54% of the Pareto-scaled dataset-wide variance. (b,d) The loading plot on the right of the respective datasets demonstrates the weights of each individual metabolite that contributes to the separation of samples on the left scores plot. GC, gas chromatography; MS, mass spectrometry; O, uniform ovoid; OT, heterogeneous ovoid and tubular; S, uniform spherical; SO, heterogeneous spherical and ovoid; T, uniform tubular; TMS, trimethylsilyl; UPLC, ultra performance liquid chromatography

in Figure 3 and reported in Table S3. Of these significantly differing compounds, 12 GC–MS and 27 UPLC–MS compounds were annotated. From these 39 compounds, 19 metabolites with literature-based evidence for potential relevant connections to embryonic developmental biology were more thoroughly investigated (Table 1).

2.3 | MetScape 3 analysis

After selection of significant metabolites by one-way ANOVA tests, 19 compounds with potential roles in preimplantation embryo development were inputted into MetScape 3 for pathway analysis. Figure 4 illustrates the generated pathway-based network of the selected compounds in five categories of related metabolites: amino acid metabolism (β-alanine, glycine, phenylalanine, serine, tryptophan, 5-hydroxy-L-tryptophan, and tyrosine); bile metabolism (cholesterol, ethanolamine, hexadecasphinganine, and phosphoric acid); protein catabolism (2-methylbutyryl-L-carnitine, agmatine, *N*-acetylglutamic acid, and urea); purine catabolism (uric acid and xanthine); and energy catabolism (butyryl-L-carntine and creatinine). Of the 19 selected compounds, 10 compounds (i.e., β-alanine, phenylalanine, serine, ethanolamine, hexadecasphinganine, 2-methylbutyryl-L-carnitine, *N*-acetylglutamic acid, urea, butyryl-L-carnitine, and creatinine) had significantly increasing ($p < .05$) concentrations in the uterine lumen as elongation of respective conceptuses progressed from pre-elongation stage through the transitional stages (Figure 5). In contrast, the remaining nine compounds (i.e., 5-hydroxy-L-tryptophan, glycine, tryptophan, tyrosine, cholesterol, phosphoric acid, agmatine, uric acid, and xanthine) followed the reverse trend and significantly decreased ($p < .05$) from pre-elongation through the transitional stages (Figure 5). Significant differences in metabolite concentrations in uterine flushings between each corresponding conceptus morphology were explored within the five metabolite categories in the following sections.

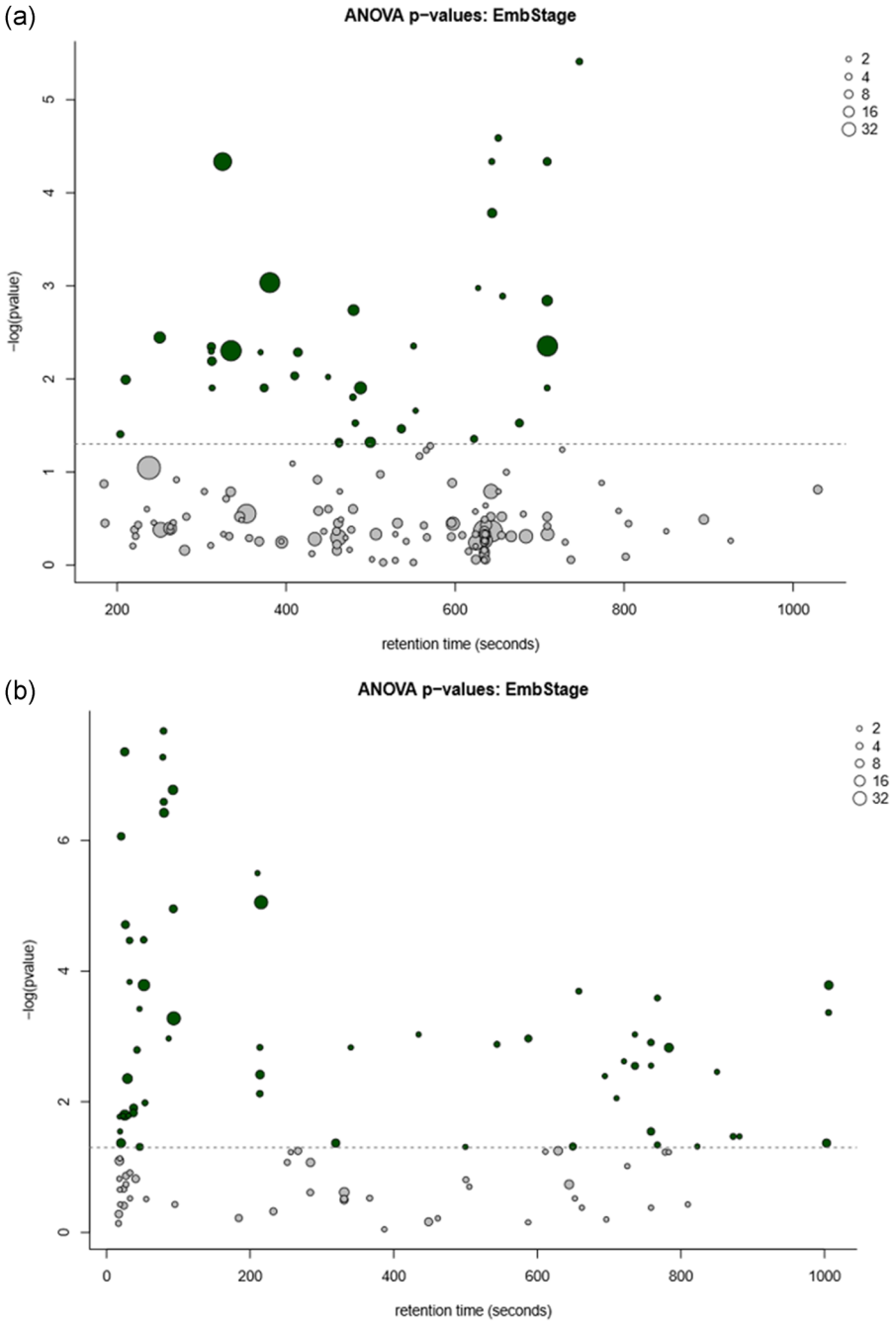

FIGURE 3 (a) GC–MS and (b) UPLC–MS ANOVA bubble plots of compounds separating uterine flushings by the effect of conceptus morphology present. This plot depicts the *p* value for each metabolite and factor on the –log10 scale (*y*-axis). The *x*-axis represents retention time. Point size reflects the number of mass features for each compound, an approximation of signal intensity, and spectrum complexity. All colored points above the dotted line are deemed significantly differing in abundance based on treatment group after FDR correction at $p < .05$ level among uterine flushings containing one of the five conceptus morphology treatment groups (i.e., S, SO, O, OT, or T). ANOVA, analysis of variance; FDR, false discovery rate; GC, gas chromatography; MS, mass spectrometry; O, uniform ovoid; OT, heterogeneous ovoid and tubular; S, uniform spherical; SO, heterogeneous spherical and ovoid; T, uniform tubular; UPLC, ultra performance liquid chromatography

2.4 | Amino acid metabolism

From the MetScape metabolite network, 7 of the 19 compounds were identified as amino acids (Figure 6). There was a significant increase in serine levels from uterine milieu containing the first two morphologies (i.e., S and SO) to the later three morphologies (i.e., O, OT, and T). Similarly, β-alanine levels of uterine flushings increased from S and SO morphologies to the uterine flushings of the later two morphologies (i.e., OT and T), and phenylalanine flushings levels significantly increased from S and SO to the last morphology flushings (i.e., T). Conversely, there was a significant decrease both in glycine and tyrosine abundance between uterine flushings during the pre-elongation stage (i.e., S) and all subsequent stages (i.e., SO, O, OT, and T). Tryptophan and its derivative 5-hydroxy-L-tryptophan significantly decreased in uterine flushings abundance after the pre-elongation stage (i.e., S) and also from the early initiation stage (i.e., SO) to the transitional stages (i.e., OT and T).

2.5 | Bile metabolism

From the MetScape metabolite network, there were four compounds that were classified as being involved in bile metabolism

TABLE 1 Selected metabolites detected by GC–MS or UPLC–MS with potential roles as endogenous metabolites that changed ($p < .05$) in uterine milieu during the early stages of porcine blastocyst elongation

Annotated compound	*p* Value	Score	Retention time, s	Method
2-Methylbutyryl-L-carnitine	.001075242	2	86.1205	UPLC–MS
5-Hydroxy-L-tryptophan	5.34E−08	2	77.96667	UPLC–MS
β-Alanine (3TMS)	.005168837	2	413.4124	GC–MS
Agmatine	.042832436	2	19.4304	UPLC–MS
Butyryl-L-carnitine	.001610562	2	41.8635	UPLC–MS
Cholesterol	.002401609	2	720.258	UPLC–MS
Creatinine (3TMS)	.001821255	2	479.137	GC–MS
Ethanolamine (3TMS)	.006441812	2	311.6718	GC–MS
Glycine (2TMS)	.003585729	2	249.8665	GC–MS
Hexadecasphinganine	.00147265	2	339.8155	UPLC–MS
N-Acetylglutamic acid	.000378459	2	45.5115	UPLC–MS
Phenylalanine	.049042744	2	45.7008	UPLC–MS
Phosphoric acid (3TMS)	.004983105	2	333.6724	GC–MS
Serine (2TMS)	4.62188E−05	2	323.8715	GC–MS
Tryptophan	3.78E−07	2	79.3871	UPLC–MS
Tyrosine	3.39597E−05	2	31.51725	UPLC–MS
Urea (2TMS)	.004506316	2	311.053	GC–MS
Uric acid (4TMS)	.004432358	2	707.9329	GC–MS
Xanthine (3TMS)	.029778532	2	675.5724	GC–MS

Abbreviations: GC, gas chromatography; MS, mass spectrometry; TMS, trimethylsilyl; UPLC, ultra performance liquid chromatography.

that significantly changed in the uterine milieu as blastocysts transitioned through the early stages of elongation (Figure 7). For instance, the level of cholesterol significantly decreased from uterine flushings during the pre-elongation stage (i.e., S) to the later initiation and transitional stages (i.e., O, OT, and T). Phosphoric acid uterine flushing abundance experienced a significant decrease from the first early stages (i.e., S, SO, and O) to later transitional stages (i.e., OT and T). In contrast, ethanolamine levels increased significantly from uterine flushing during the pre-elongation and early initiation stages (i.e., S and SO) to the later transitional stages (i.e., OT and T). Lastly, the abundance of hexadecasphinganine in uterine flushings significantly increased between S morphology and both heterogeneous population morphologies (i.e., SO and OT).

2.6 | Protein catabolism

From the MetScape metabolite network, 4 of the 19 compounds were classified as components of protein and amino acid catabolism (Figure 8). Agmatine abundance in uterine flushings significantly decreased between SO and T morphologies. Uterine flushings abundance of both urea and 2-methylbutyryl-L-carnitine significantly increased from S and SO morphologies to O, OT, and T morphologies. *N*-acetylglutamic acid flushings levels significantly increased between S morphology and all subsequent morphologies (i.e., SO, O, OT, and T).

2.7 | Purine catabolism

From the MetScape metabolite network (Figure 4), 2 of the 19 compounds were categorized as products of the catabolism of purines (Figure 8). Uterine flushings levels of xanthine significantly decreased between S morphology and all subsequent morphologies (i.e., SO, O, OT, and T). Similarly, uric acid levels in flushings significantly decreased from S and SO morphologies to O, OT, and T morphologies.

2.8 | Energy catabolism

From the MetScape metabolite network (Figure 4), 2 of the 19 compounds were categorized as products of the catabolism of energetic sources (Figure 8). Both butyryl-L-carnitine and creatinine significantly increased in uterine flushings from S morphology to O, OT, and T morphologies. Additionally, there was a significant increase in butyryl-L-carnitine flushings levels from SO to OT and T morphologies.

3 | DISCUSSION

The objective of the current study was to identify metabolites in the uterine lumen that significantly change in concentration

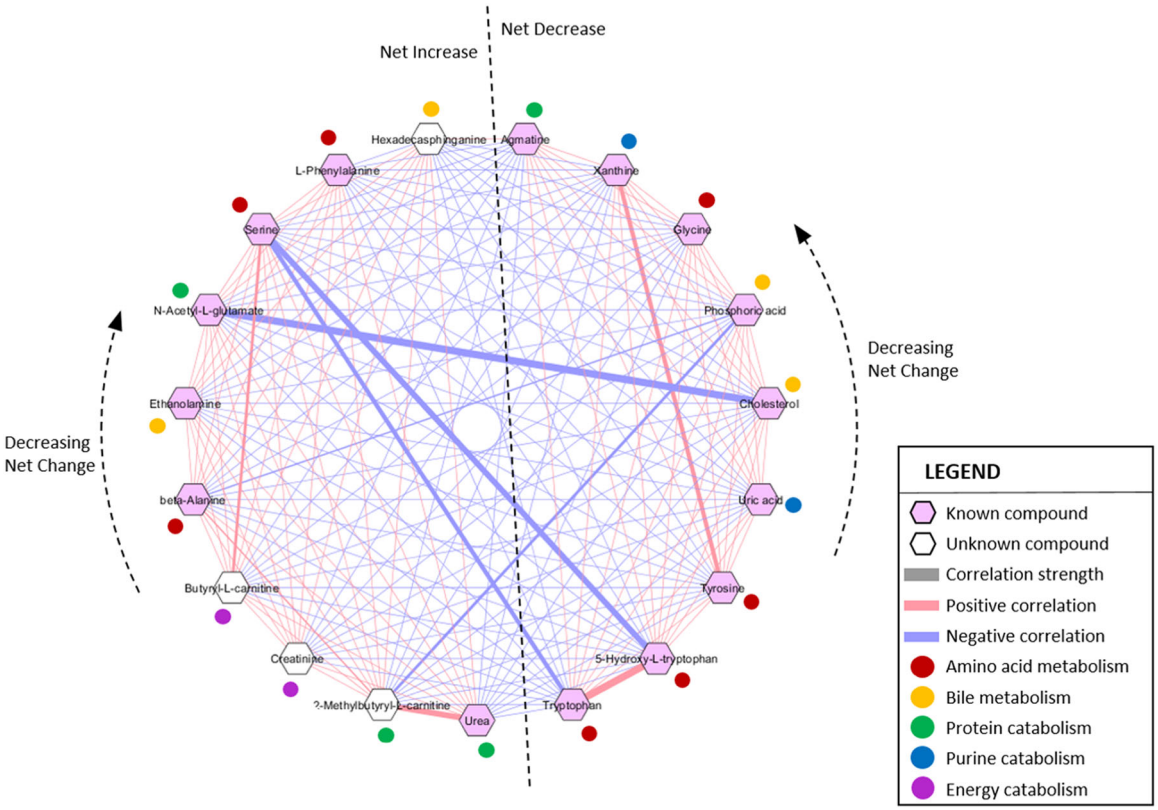

FIGURE 4 MetScape 3 correlation network of metabolites as determined by abundance changes throughout the stages of elongation. The thickness of line represents correlation strength. Metabolites to the left of the dividing line had an overall net increase in concentration throughout the elongation stages; starting with the metabolite at the bottom (urea) and moving clockwise to the top (hexadecasphinganine), the total change in concentration for each metabolite across elongation stages decreases. For example, urea had the highest overall increase over time, while hexadecasphinganine had the lowest overall increase. Metabolites to the right of the dividing line had an overall net decrease in concentration throughout elongation; total concentration change decreases moving counterclockwise from tryptophan to agmatine

between early stages of porcine conceptus elongation through GC–MS and UPLC–MS analyses. The identified annotated metabolites were then screened with an extensive literature search for possible functional relevance to preimplantation embryo development to hypothesize potential rationales for the observed trends in changing metabolite concentrations as they relate to early porcine conceptus elongation. On the basis of this screen, 19 compounds, 10 of which exhibited a significant increase and 9 that exhibited a significant decrease in the uterine milieu over the progression of elongation, were explored for potential involvement in conceptus growth and development as well as potential to adversely affect conceptus development throughout elongation. Overall, the results of this study illustrate the importance of temporal regulation of the uterine environment to promote the initiation of porcine conceptus elongation and subsequent endometrial implantation by identifying specific metabolic compounds exhibiting differences in uterine milieu abundance corresponding to conceptus morphology throughout the early stages of porcine conceptus elongation.

3.1 | Amino acid metabolism

One outcome of this study was the emergence of different patterns of amino acid abundance in the uterine fluid across different early stages of porcine elongation. Although the presence of amino acids available for uptake have been shown to influence preimplantation embryo development (Humpherson, Leese, & Sturmey, 2005), the many metabolic processes in which each amino acid can participate has prevented a clear link to specific pathways or the mechanisms involved. In the current study, the sustained increase in serine and β-alanine uterine luminal abundance after the first stages (i.e., S and SO) to the later transitional stages (i.e., OT and T) of elongation was accompanied by a corresponding sustained decrease in glycine after the pre-elongation stage (i.e., S) compared with later stages (i.e., SO, O, OT, and T). It is possible that the rise in serine abundance of uterine flushings allows an increase in conceptus utilization of serine as a carbon donor in one-carbon metabolism (Kalhan & Hanson, 2012), potentially contributing to the cell growth and proliferation important in the later stages of pig blastocyst

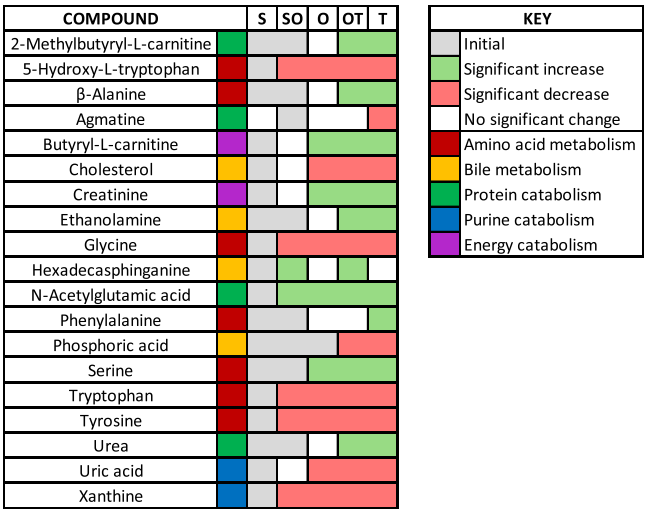

FIGURE 5 Trends in significant metabolite abundance changes of uterine flushings over the progression of blastocyst early elongation. Gray boxes represent initial metabolite abundance; green boxes represent a significant increase in metabolite abundance, while red boxes represent a significant decrease in metabolite abundance at the corresponding conceptus morphologies. Colors next to the metabolite name classify metabolites into categories of related metabolites. O, uniform ovoid; OT, heterogeneous ovoid and tubular; S, uniform spherical; SO, heterogeneous spherical and ovoid; T, uniform tubular

elongation (L. Blomberg, Hashizume, & Viebahn, 2008). It has been shown that the rapid proliferation of many cells is dependent on an abundance of exogenous serine, as donation of one-carbon units by serine during one-carbon metabolism is critical in the function and regulation of many cellular processes including synthesis of metabolic intermediates, amino acids, nucleotides, and phospholipids, as well as methylation of proteins, DNA, and RNA (Kalhan & Hanson, 2012). Conversely, the temporal decrease in glycine levels within uterine flushings seen here in this study could be due to the abundance of serine available for uptake, as glycine can be synthesized intracellularly from serine during the process of one-carbon metabolism. In fact, it has been suggested that although serine conversion to glycine is essential in rapid cell proliferation, an excess of glycine itself can inhibit this proliferation (Shuvalov et al., 2017). Multiple studies of preimplantation mouse embryo development have indicated a decrease in the activity of the specific glycine transport system as embryos reach the blastocyst stage (Khatchadourian, Guillaud, & Menezo, 1994; Richards, Wang, Liu, & Baltz, 2010; Van Winkle, Haghighat & Campione, 1990), possibly providing support to the hypothesis that blastocyst uptake of glycine decreases during elongation. Additionally, it is possible that during elongation, the conceptus decreases the metabolism of glycine as an energy substrate and begins to utilize glycine for intracellular conversion into proteins and purines, as metabolism of glycine as an energy substrate decreases and glycine conversion into amino acids as well as incorporation into proteins and purines increases as mouse embryos reach the blastocyst stage (Khatchadourian et al., 1994). Although both glycine and β-alanine possess the ability to function as osmolytes for the protection of early embryos during development (Hammer & Baltz, 2003; Richards et al., 2010), β-alanine will only adopt this role when glycine abundance is low (Hammer & Baltz, 2003). Thus, it is possible the rise in β-alanine levels in luminal fluid observed in the current study after the pre-elongation and early initiation stages (i.e., S and SO) is to increase availability for utilization as an osmolyte for the protection of the blastocyst in the later elongation stages as glycine levels decrease and its metabolism shifts to incorporation into macromolecules.

Two other amino acids found in the current study to change in concentration over the progression of elongation, phenylalanine and tyrosine, are commonly incorporated into pig preimplantation embryo culture media for consumption by developing blastocysts (Chen et al., 2018; Gardner, 1998; Krisher et al., 2015; Li et al., 2007). While phenylalanine abundance in the uterine lumen was found to rise in the current study from the early stages (i.e., S and SO) to the final transitional stage (i.e., T) of elongation, tyrosine levels had a corresponding decrease in abundance after the pre-elongation stage (i.e., S). Phenylalanine supplementation to the blastocyst may temporally increase over the course of elongation to meet the increasing demand for protein and amino acid synthesis and conversion to tyrosine, as protein synthesis has been identified as one of the major classical pathways and most significant biological functions occurring during the later ovoid, tubular, and filamentous stages of porcine blastocyst elongation (L. Blomberg et al., 2008). Additionally, studies have shown that protein synthesis increases throughout murine preimplantation embryo development to the blastocyst stage (Houghton, Thompson, Kennedy, & Leese, 1996; Sturmey, Reis, Leese, & McEvoy, 2009). Though both phenylalanine and tyrosine are required for the synthesis of proteins, only phenylalanine is considered essential due to the ability of tyrosine to be readily synthesized from phenylalanine (D'Mello, 2003). As such, a lower supply of tyrosine can be compensated for by an increase in phenylalanine, though the reverse is not true (D'Mello, 2003). However, since both are necessary for proper cellular function, only a part of the phenylalanine supply can be converted to tyrosine, suggesting the need for an increase in total phenylalanine supplementation (D'Mello, 2003), as was observed in the current study.

In the current study, tryptophan and 5-hydroxy-L-tryptophan significantly decreased in the uterine lumen from the pre-elongation stage (i.e., S) to the initiation stage (i.e., SO), and then again from SO morphology to the transitional stages (i.e., OT and T). This decrease in tryptophan and 5-hydroxy-L-tryptophan, an intermediate in the conversion of tryptophan to serotonin, over the early progression of elongation may be due to the breakdown of tryptophan into kynurenine and other kynurenine pathway metabolites to serve as a mechanism of immunoregulation for semiallogeneic fetal tolerance at the time of blastocyst implantation. Tryptophan catabolism by the kynurenine pathway is

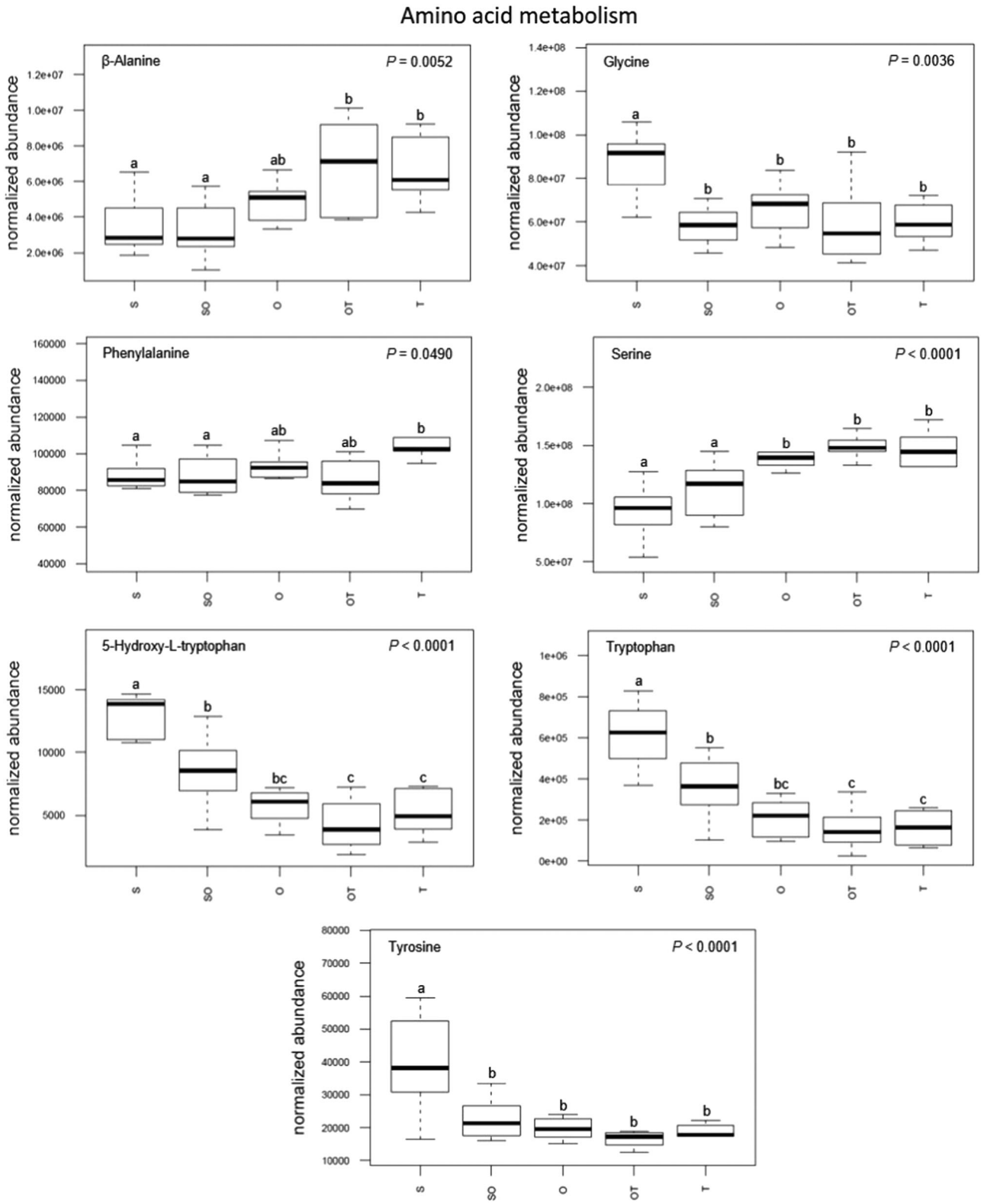

FIGURE 6 Changes in metabolite concentrations associated with amino acid metabolism within the uterine milieu throughout the progression of early porcine blastocyst elongation. Uterine flushings were categorized through this progression based on the morphology of recovered conceptuses as uniform spherical (S), heterogeneous spherical and ovoid (SO), uniform ovoid (O), heterogeneous ovoid and tubular (OT), or uniform tubular (T). Box plot depicts the influence of blastocyst treatment on the normalized abundance of the metabolites within corresponding uterine flushings with complete model *p* value depicted on the top right. Box plots with different letters differ significantly ($p < .05$)

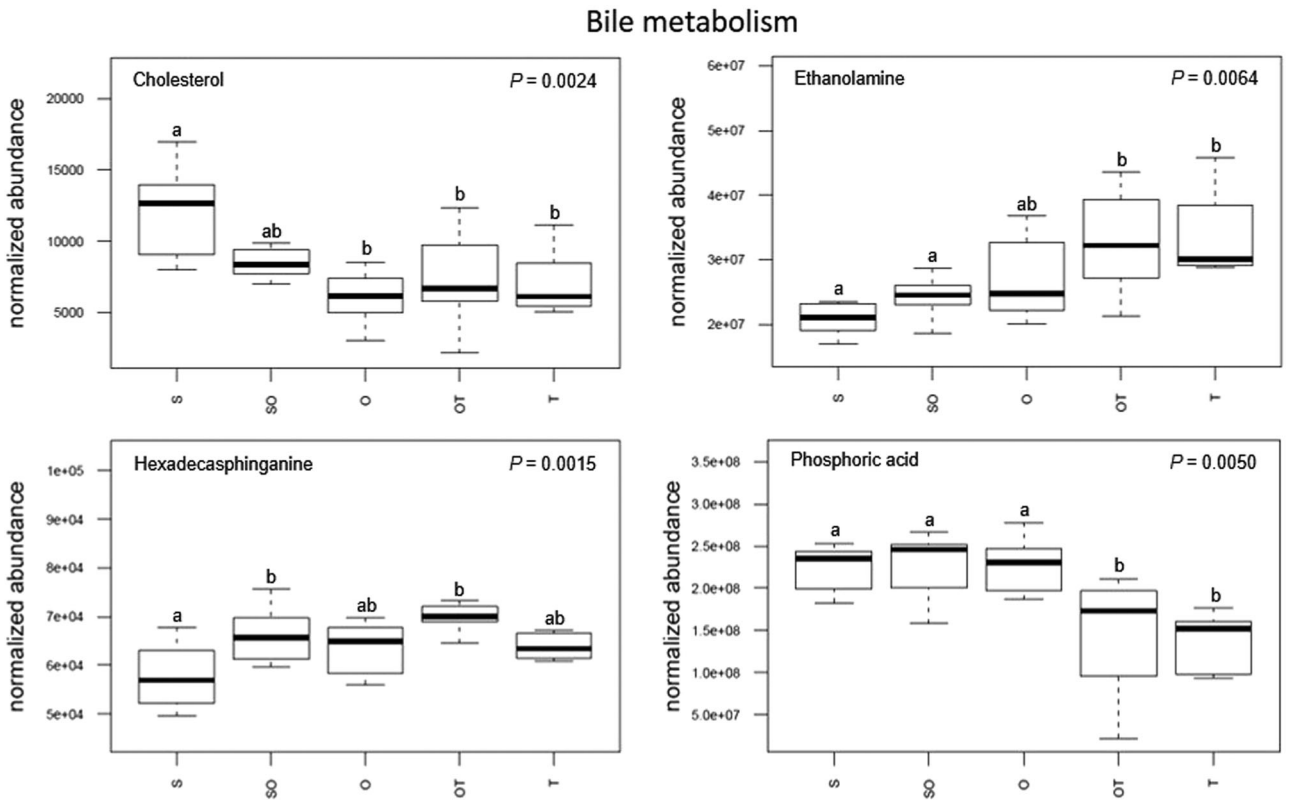

FIGURE 7 Changes in metabolite concentrations associated with bile metabolism within the uterine milieu throughout the progression of early porcine blastocyst elongation. Uterine flushings were categorized through this progression based on the morphology of recovered conceptuses as uniform spherical (S), heterogeneous spherical and ovoid (SO), uniform ovoid (O), heterogeneous ovoid and tubular (OT), or uniform tubular (T). Box plot depicts the influence of blastocyst treatment on the normalized abundance of the metabolites within corresponding uterine flushings with complete model *p* value depicted on the top right. Box plots with different letters differ significantly ($p < .05$)

catalyzed by the interferon-γ (IFNG)-induced activation of indoleamine 2,3-dioxygenase (IDO) (Moffett & Namboodiri, 2003; Wichers & Maes, 2004). IFNG is the main interferon produced by the porcine trophoblast, and is synthesized and secreted at high amounts between Days 12–20 of gestation at the time of endometrial attachment (Mathew, Lucy & Geisert, 2016; Murphy et al., 2009). This interferon moves across the uterine lumen to exert effects on the maternal endometrium to promote successful blastocyst implantation, likely acting in part to induce IDO activity for the catabolism of tryptophan to produce immunomodulation for semiallogeneic fetal tolerance (Murphy et al., 2009).

3.2 | Bile metabolism

Cholesterol levels in the uterine lumen during the current study significantly decreased from the pre-elongation stage (i.e., S) to the late initiation and transitional stages (i.e., O, OT, and T). These results are supported by similar findings in a study performed by Samborski, Graf, Krebs, Kessler, and Bauersachs (2013), which reported decreased endometrial expression of genes involved in cholesterol biosynthesis in the late stages of porcine elongation (Samborski et al., 2013). The decrease in luminal cholesterol seen in the current study could be related to the utilization of cholesterol for uterine epithelial cell proliferation or the essential maternal production of hormones during this preimplantation period (Baardman et al., 2013). A study by Lobo et al. (2009) detected an increase in hormone-sensitive lipase, an intracellular lipase that hydrolyzes stored cholesterol for use in cellular processes and hormone synthesis, in rat uterine epithelial cells at the later stages of estrus, possibly indicating uterine epithelial cell proliferation or the maternal biosynthesis of hormones from cholesterol during the preimplantation stages of pregnancy (Lobo et al., 2009). Furthermore, Meier, Trewhella, Fairclough, and Jenkin (1997) detected a decrease in endometrial signaling lipid precursor concentrations corresponding to the initiation of elongation in early ewe pregnancy (Meier et al., 1997), further supporting the results of the current study. Another possible explanation for the decrease in cholesterol observed in this study is the increasing ability of the fetus to utilize endogenous sources for synthesis of cholesterol and precursor molecules throughout the progression of development, which could correspond to decreasing maternal cholesterol secretion for embryonic uptake.

Other metabolites involved in bile metabolism include ethanolamine and hexadecasphinganine, both of which exhibited a significant increase in luminal fluid concentration in the transitional stages of elongation (i.e., T) in the current study. This increase could be due to

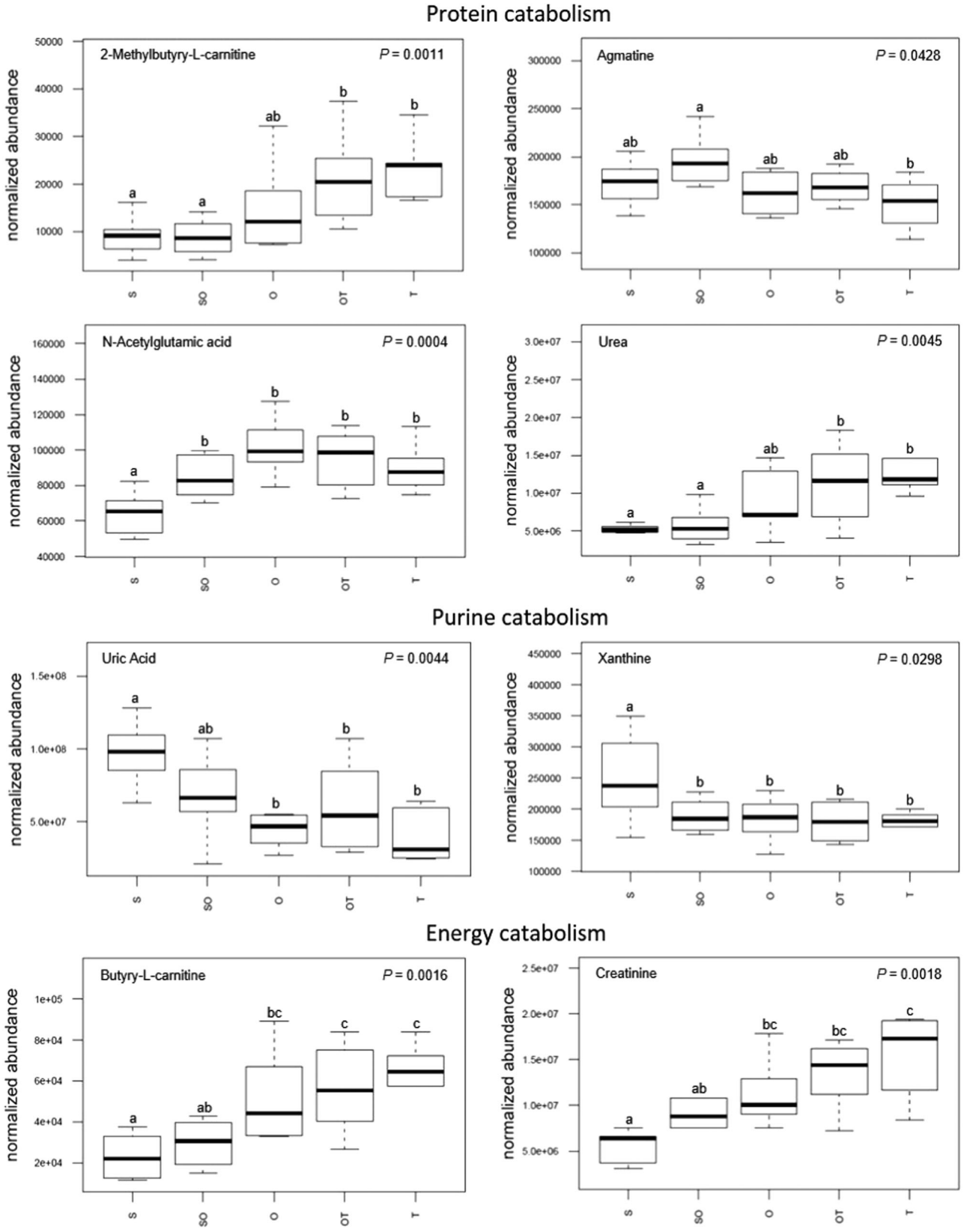

FIGURE 8 Changes in metabolite concentrations associated with the catabolism of protein, purine, and energy within the uterine milieu throughout the progression of early porcine blastocyst elongation. Uterine flushings were categorized through this progression based on the morphology of recovered conceptuses as uniform spherical (S), heterogeneous spherical and ovoid (SO), uniform ovoid (O), heterogeneous ovoid and tubular (OT), or uniform tubular (T). Box plot depicts the influence of blastocyst treatment on the normalized abundance of the metabolites within corresponding uterine flushings with complete model p value depicted on the top right. Box plots with different letters differ significantly ($p < .05$)

the rapid cell growth and proliferation occurring during the progression of conceptus elongation, as these compounds are essential components of these processes. More specifically, ethanolamine has been shown to stimulate the rapid growth of mammalian cells, likely due to the stimulation of phosphatidylethanolamine (PE) synthesis (Patel & Witt, 2017). PE functions to stabilize membrane-anchored proteins as well as participate in cell division, fusion, and apoptosis following incorporation into cell membranes (Fullerton, Hakimuddin, & Bakovic, 2007). Studies have shown that Pcyt2, an essential gene for the synthesis of PE from ethanolamine, is necessary for the development of murine embryos as embryonic lethality results from its complete knockout and inability to synthesize PE from ethanolamine, providing evidence for the importance of available ethanolamine during development (Fullerton et al., 2007). Hexadecasphinganine falls into the class of sphingolipids, which have major roles in signaling to regulate important cellular processes including cell proliferation, metabolism, differentiation, and protein synthesis (Adan-Gokbulut, Kartal-Yandim, Iskender, & Baran, 2013). In support of the present findings, an increase in sphingolipid metabolism, specifically in sphingolipid-based extracellular membrane compounds, has been identified in the porcine uterine epithelium at the later stages of elongation, suggesting a potential role in trophoblast elongation or attachment (Kayser, Kim, Cerny, & Vallet, 2006).

3.3 | Protein catabolism

The urea level in the uterine lumen significantly increased from the pre- and initial stages of elongation (i.e., S and SO) to the final transitional stages (i.e., OT and T) in the current study. Similarly, luminal *N*-acetylglutamic acid significantly increased between the pre-elongation stage (i.e., S) and all subsequent stages (i.e., SO, O, OT, and T). As both metabolites are part of the urea cycle, a metabolic endpoint in the catabolism of amino acids (Caldovic et al., 2010; Nelson & Cox, 2013), and indicators of protein catabolism (Saheki, Katsunuma, & Sase, 1977; Salazar, 2014), these results may suggest an increase in amino acid and protein catabolism over the progression of porcine conceptus elongation, possibly to reutilize amino acids for protein synthesis or for amino acid consumption as a fuel source (Nelson & Cox, 2013). Further evidence of increased amino acid catabolism in the transitional stages of elongation was the uterine luminal increase of 2-methylbutyryl-L-carntine, a by-product in the catabolism of isoleucine (Gibson et al., 2000), observed in this study between the pre-elongation and early initiation stages (i.e., S and SO) and the transitional stages (i.e., OT and T).

Agmatine concentrations in uterine flushings decreased significantly between the initiation stage of elongation (i.e., SO) and the final transitional stage (i.e., T) in the current study. Agmatine is a product of the decarboxylation of arginine and can be converted to putrescine to generate polyamines, and has also been shown to be a competitive inhibitor of nitric oxide (NO) synthases in the production of NO (Galea, Regunathan, Eliopoulos, & Feinstein, 1996). NO uterine generation has been shown to be upregulated during pregnancy, and it has been suggested that NO has a role in the implantation process (Biswas, Kabir, & Pal, 1998). Estrogen stimulates NO generation through the induction of arginine, and it has been hypothesized that NO acts as an effector molecule for mediation of the uterine effects of estrogen, possibly through vasoregulation (Biswas et al., 1998). A study by Biswas et al. (1998) showed that the inhibition of NO synthase significantly inhibited implantation of rat blastocysts (Biswas et al., 1998). Thus, it is possible that the late-stage decrease in luminal agmatine is associated with the need for effective NO production to help facilitate subsequent conceptus implantation.

3.4 | Purine catabolism

The uric acid concentration in uterine flushings significantly decreased after the pre-elongation and early initiation stages (i.e., S and SO) for the remaining transitional stages of elongation in the current study. Similarly, uterine luminal xanthine decreased significantly after the pre-elongation stage (i.e., S). These results may suggest a decrease in the catabolism of purines in the later stages of porcine conceptus elongation, as purines are catabolized to xanthine and finally converted into uric acid (Dienhart, O'Brien, & Downs, 1997; Maiuolo, Oppedisano, Gratteri, Muscoli, & Mollace, 2016). Purine nucleotides are essential during rapid cell division, as they are incorporated into DNA and RNA and function as coenzymes in bioenergetic processes (Dienhart et al., 1997), offering a potential explanation for the decrease of purine catabolism as elongation progresses.

3.5 | Energy catabolism

In the current study, the concentration of creatinine in the uterine lumen significantly increased from the pre-elongation stage (i.e., S) to the late initiation and transitional stages of elongation (i.e., O, OT, and T). Creatinine is the breakdown product of creatine and phosphocreatine (Salazar, 2014), and therefore relates to the amount of creatine being used by cellular processes (Matsuo et al., 2009). The interconversion of these latter two compounds by creatine kinase (CK) functions as an energy storage and release mechanism for rapid ATP generation in times of high energy demand (Forsey, Ellis, Sargent, Sturmey, & Leese, 2013; Yan, 2016). Many ATP-related cellular processes have high energy demands, such as cell signaling, mitosis, and cell movement (Yan, 2016). Studies have shown the function of CK in cell motility and mitosis processes and determined its necessity for the ATP-functioning mitosis apparatus (Yan, 2016). Additionally, rapidly dividing cells utilize glycolysis as the main source of ATP production, and CK associates with enzymes of this pathway (Yan, 2016). A study by Forsey et al. (2013) demonstrated the presence of CK protein and

gene expression throughout mouse preimplantation embryo development, suggesting the role of the creatine-phosphate pathway as a potential source of ATP (Forsey et al., 2013). The findings of these previous studies align with the temporal increase of creatine metabolism during early porcine blastocyst elongation observed in this study. Additionally, as butyryl-L-carnitine is a by-product of long-chain fatty acid β-oxidation (Nochi, Olsen, & Gregersen, 2017), the significant uterine luminal increase of butyryl-L-carnitine from the pre-elongation stage (i.e., S) to the late initiation and transitional stages (i.e., O, OT, and T) in this study may suggest an increase in conceptus fatty acid catabolism after the initiation of elongation, providing support to the hypothesis of an overall increase in catabolism of energy substrates to supply the energy-demanding cellular processes occurring during the early stages of porcine embryo elongation.

In conclusion, the results of this study offer insights into the changing uterine lumen metabolite concentrations native to the pig throughout the initiation and early transition of blastocyst elongation. Metabolomic analysis of uterine flushings over the progression of porcine conceptus elongation allowed for observations of temporal metabolite trends associated with specific elongation stages, correlating to uniform spherical, uniform ovoid, and uniform tubular stage populations, as well as the heterogeneous spherical/ovoid and ovoid/tubular populations. Amino acid, bile, protein, purine, and energy metabolism groups of associated metabolites exhibited both significant increase and decrease throughout the initiation and transition progression of blastocyst elongation, and potential rationales for observed trends were explored. A limitation of the current study is the inability to determine with certainty the source of an observed change in metabolite levels of the uterine flushings, as this change could be due to an alteration in uterine/conceptus secretion or uptake. Therefore, interpretations of the observed changes in metabolite levels can only be hypothesized based on the known functions and abundance changes of individual and related compounds as well as conclusions drawn from related studies found in the literature. In the future, we plan to provide further evidence for these hypotheses through global transcriptome analysis of corresponding conceptus morphologies throughout these early elongation stages. Therefore, the information gained in this study may offer more insight into the specific mechanisms involved in this essential period of porcine preimplantation conceptus development.

4 | MATERIALS AND METHODS

4.1 | Animal, sample collection, and sample preparation

All animal protocols were approved by the U.S. Meat Animal Research Center (USMARC) Institutional Animal Care and Use Committee (EO3040-31000091-04). Procedures for handling animals complied with the Guide for the Care and Use of Agricultural Animals in Research and Teaching (FASS, 2010). Postpubertal White cross-bred gilts consisting of Landrace, Yorkshire, and Duroc genetics were checked daily for estrus. Following the first detection of estrus (designated as Day 0), gilts were artificially inseminated with semen from pooled terminal Duroc sires collected from a commercial boar stud and again 24 hr later with the same pool of semen. Over a 1-year collection period, 38 pregnant gilts were harvested at the USMARC abattoir on Days 9, 10, or 11 of gestation. Immediately after the gilts had been harvested, their reproductive tracts were removed and each uterine horn was flushed with 20 ml of 25 mM 4-(2-hydroxyethyl)-1-piperazineethanesulfonic acid-buffered Roswell Park Memorial Institute-1640 medium (Thermo Fisher Scientific, Waltham, MA; ~37°C) containing 1X antibiotics/antimycotics (MilliporeSigma, St. Louis, MO). Blastocysts were recovered and classified into embryo stages according to size and morphology using a standard stereomicroscope (Nikon Instruments, Melville, NY): spherical (~1 mm), ovoid (3–9 mm), or tubular (>10 mm). Uterine flushings from each uterine tract were collected, centrifuged at 2100*g* for 20 min at 4°C to remove cellular debris, and stored separately at −80°C until GC–MC or UPLC–MS analysis. Uterine flushing samples were classified into populations based on conceptus morphologies of corresponding litters illustrated in Figure 1 as: uniform spherical (S, $n = 8$ gilts), heterogeneous spherical and ovoid (SO, $n = 8$ gilts), uniform ovoid (O, $n = 8$ gilts), heterogeneous ovoid and tubular (OT, $n = 8$ gilts), or uniform tubular (T, $n = 6$ gilts). The uterine flushing of a litter was classified as uniform if at least 80% of conceptuses in the respective litter were of the same morphological classification of the latest stage morphology, due to the difficulty of obtaining 100% homogeneous tubular morphologies (Figure 1). An aliquot of sample (100 µl) was mixed with 100 µl of acetonitrile and incubated at −20°C overnight, and then centrifuged at 17,000*g* for 15 min at 4°C. From this supernatant, 30 µl was dried down for GC–MS and 100 µl of supernatant was dried down for UPLC–MS.

4.2 | GC–MS analysis

Dried samples were resuspended in 50 µl of pyridine containing 25 mg/ml of methoxyamine hydrochloride, incubated at 60°C for 45 min, vigorously vortexed for 30 s, sonicated for 10 min, and incubated for an additional 45 min at 60°C. Next, 50 µl of *N*-methyl-*N*-trimethylsilyltrifluoroacetamide with 1% trimethylchlorosilane (Thermo Fisher Scientific) was added, and samples were vigorously vortexed for 30 s and incubated at 60°C for 30 min. Metabolites were detected using a Trace 1310 GC coupled to a Thermo ISQ mass spectrometer. Samples (1 µl) were injected at a 10:1 split ratio to a 30 m TG-5MS column (Thermo Fisher Scientific; 0.25 mm id, 0.25 µm film thickness) with a 1.2 ml/min helium gas flow rate. The GC inlet was held at 285°C. The oven program started at 80°C for 30 s, followed by a ramp of 15°C/min to 330°C, and an 8 min hold. Masses between 50 and 650 m/z were scanned at 5 scans/s under electron impact ionization. Transfer line and ion source were held at 300°C and 260°C, respectively. Pooled quality control (QC) samples were

injected after every six actual samples. The analytical sample order was randomized.

4.3 | UPLC–MS analysis

Extracts were resuspended in 50 µl of 70% methanol and 30% water. Samples were injected (3 µl) onto a Waters Acquity UPLC system (Waters Corporation, Milford, MA) in discrete, randomized blocks, and separated using a Waters Acquity UPLC CSH Phenyl Hexyl column (1.7 µM, 1.0 × 100 mm), using a gradient from solvent A (water, 0.1% formic acid) to solvent B (Acetonitrile, 0.1% formic acid). Injections were made in 100% A, held at 100% A for 1 min, ramped to 98% B over 12 min, held at 98% B for 3 min, and then returned to starting conditions over 0.05 min and allowed to re-equilibrate for 3.95 min, with a 200 µl/min constant flow rate. The column and samples were held at 65°C and 6°C, respectively. The column eluent was infused into a Waters Xevo G2 Q-Tof-MS (Waters Corporation) with an electrospray source in positive mode, scanning 50–2,000 m/z at 0.2 s per scan, alternating between MS (6 V collision energy) and MSE mode (15–30 V ramp). Calibration was performed using sodium iodide with 1 ppm mass accuracy. The capillary voltage was held at 2,200 V, source temperature at 150°C, and nitrogen desolvation temperature at 350°C with a flow rate of 800 L/hr. Pooled QC samples were injected after every six actual samples. Analytical sample order was randomized.

4.4 | Nontargeted data acquisition (GC–MS and UPLC–MS)

For each sample, raw data files were converted to .CDF format, and matrix of molecular features as defined by retention time and mass (m/z) was generated using XCMS software in R (Smith, Want, O'Maille, Abagyan, & Siuzdak, 2006) for feature detection and alignment. The matched-filter algorithm was used for GC–MS data, and the centWave algorithm for UPLC–MS data. Features were grouped using RAMClustR (Broeckling, Afsar, Neumann, Ben-Hur, & Prenni, 2014), with options set as hmax = 0.7, minModuleSize = 2, linkage = "average," and normalize = "quantile" for GC–MS data, and hmax = 0.3, linkage = "average," normalize = "TIC," and minModuleSize = 2 for UPLC–MS data.

GC–MS spectra were annotated by matching unknown spectra to the Golm metabolome retention indexed spectral library (Kopka et al., 2004), using retention times plotted versus the Golm retention index to increase confidence in the spectral match. Searching was accomplished using the RAMSearch program (Broeckling et al., 2016). Additional GC–MS matching was performed by searching against the NIST v12 EI spectral database.

UPLC–MS data were first annotated by searching against an in-house spectra and retention time database using RAMSearch. RAMClustR was used to call the findMain (Jaeger, Meret, Schmitt, & Lisec, 2017) function from the interpretMSSpectrum package to infer the molecular weight of each UPLC–MS compound and annotate the mass signals. The complete MS spectrum and a truncated MSE spectrum were written to a .MAT format for import to MSFinder (Tsugawa et al., 2016). The MSE spectrum was truncated to only include masses with values less than the inferred M plus its isotope, and the .MAT file precursor ion was set to the M + H ion for the findMain inferred M value. These .mat spectra were analyzed to determine the most probable molecular formula and structure using MS-Finder console. MSFinder was also used to perform a spectral search against the MassBank database. All results were imported into R and a collective annotation was derived with prioritization of RAMSearch > MSFinder mssearch > MSFinder structure > MSFinder formula > findMain M. Annotation confidence is reported as described (Sumner et al., 2007).

4.5 | MetScape 3 analysis

The 19 selected significant metabolites were analyzed with MetScape 3 version 3.1.3 in Cytoscape version 3.7.1 to determine the pathways with which each metabolite is associated (Karnovsky et al., 2012; Shannon et al., 2003). The 19 metabolites were inputted and a pathway-based network was generated. The pathways associated with each metabolite were then utilized to sort the metabolites into related groups (i.e., amino acid metabolism, bile metabolism, protein catabolism, purine catabolism, and energy catabolism; Figure 4). The normalized abundance values of each compound were inputted into MATLAB and correlation values were obtained for each pairwise relationship using the corr2 function (MATLAB, 2019). The correlation values were inputted to MetScape 3 and a correlation network was generated (Figure 4).

4.6 | Statistical analysis

PCA was performed on each dataset in R (R Core Team, 2017) using the pcaMethods package (Stacklies, Redestig, Scholz, Walther, & Selbig, 2007). Metabolite data were Pareto scaled before analysis. ANOVA between uterine flushings populations was performed using the lm() function in R, using the model "gen*trt," with posthoc pairwise comparisons "trt|genotype." All p values were false discovery corrected using the Benjamini–Hochberg method (Benjamini & Hochberg, 1995) using the p.adjust function in R.

ACKNOWLEDGMENTS

The authors would like to thank Shanda Watts, Mike Judy, and Dave Sypherd for technical assistance in collecting blastocysts, the USMARC swine crew for animal husbandry, the USMARC abattoir crew for assistance with harvesting gilts, Janel Nierman for secretarial assistance, and Dr Mark Boggess and Dr Gary Rohrer for critical review of the manuscript. This study was supported by USDA-NIFA-AFRI Grant Number 2017-67015-26456 and USDA-

ARS, CRIS Project 3400-31000-095-00D. The USDA requires us to provide the product information and EEO statement on publications.

CONFLICT OF INTERESTS

The authors declare that there are no conflict of interests.

ORCID

Jeremy R. Miles http://orcid.org/0000-0003-4765-8400
Lea A. Rempel http://orcid.org/0000-0002-8344-5085

REFERENCES

Adan-Gokbulut, A., Kartal-Yandim, M., Iskender, G., & Baran, Y. (2013). Novel agents targeting bioactive sphingolipids for the treatment of cancer. *Current Medicinal Chemistry*, *20*(1), 108–122.

Ao, Z., Li, Z., Wang, X., Zhao, C., Gan, Y., Wu, X., … Cai, G. (2019). Identification of amniotic fluid metabolomic and placental transcriptomic changes associated with abnormal development of cloned pig fetuses. *Molecular Reproduction and Development*, *86*(3), 278–291.

Baardman, M. E., Kerstjens-Frederikse, W. S., Berger, R. M. F., Bakker, M. K., Hofstra, R. M. W., & Plosch, T. (2013). The role of maternal-fetal cholesterol transport in early fetal life: Current insights. *Biology of Reproduction*, *88*(1), 24.

Bazer, F. W., Geisert, R. D., Thatcher, W. W., & Roberts, R. M. (1982). The establishment and maintenance of pregnancy. In D. J. A. Cole & G. R. Foxcroft (Eds.), *Control of pig reproduction* (pp. 227–252). London, England: Butterworth Scientific.

Bazer, F. W., Thatcher, W. W., Martinat-Botte, F., & Terqui, M. (1988). Conceptus development in large White and prolific Chinese meishan pigs. *Reproduction*, *84*(1), 37–42.

Bazer, F. W., Wu, G., Spencer, T. E., Johnson, G. A., Burghardt, R. C., & Bayless, K. (2009). Novel pathways for implantation and establishment and maintenance of pregnancy in mammals. *Molecular Human Production*, *16*(3), 135–152.

Benjamini, Y., & Hochberg, Y. (1995). Controlling the false discovery rate: A practical and powerful approach to multiple testing. *Journal of the Royal Statistical Society: Series B (Methodological)*, *57*(1), 289–300.

Bertoldo, M. J., Nadal-Desbarats, L., Gerard, N., Dubois, A., Holyoake, P. K., & Grupen, C. G. (2013). Differences in the metabolomic signatures of porcine follicular fluid collected from environments associated with good and poor oocyte quality. *Reproduction*, *146*(3), 221–231.

Biswas, S., Kabir, S. N., & Pal, A. K. (1998). The role of nitric oxide in the process of implantation in rats. *Reproduction*, *114*(1), 157–161.

Blomberg, L., Hashizume, K., & Viebahn, C. (2008). Blastocyst elongation, trophoblastic differentiation, and embryonic pattern formation. *Reproduction*, *135*(2), 181–195.

Blomberg, L. A., Schreier, L., & Li, R. W. (2010). Characteristics of peri-implantation porcine concepti population and maternal milieu influence the transcriptome profile. *Molecular Reproduction and Development*, *77*(11), 978–989.

Broeckling, C. D., Afsar, F. A., Neumann, S., Ben-Hur, A., & Prenni, J. E. (2014). RAMClust: A novel feature clustering method enables spectral-matching-based annotation for metabolomics data. *Analytical Chemistry*, *86*(14), 6812–6817.

Broeckling, C. D., Ganna, A., Layer, M., Brown, K., Sutton, B., Ingelsson, E., … Prenni, J. E. (2016). Enabling efficient and confident annotation of LC-MS metabolomics data through MS1 spectrum and time prediction. *Analytical Chemistry*, *88*(18), 9226–9234.

Brooks, K., Burns, G., & Spencer, T. E. (2014). Conceptus elongation in ruminants: Roles of progesterone, prostaglandin, interferon tau and cortisol. *Journal of Animal Science and Biotechnology*, *5*(1), 53.

Caldovic, L., Mew, N. A., Shi, D., Morizono, H., Yudkoff, M., & Tuchman, M. (2010). N-acetylglutamate synthase: Structure, function and defects. *Molecular Genetics and Metabolism*, *100*, S13–S19.

Chen, P. R., Redel, B. K., Spate, L. D., Ji, T., Salazar, S. R., & Prather, R. S. (2018). Glutamine supplementation enhances development of in vitro-produced porcine embryos and increases leucine consumption from the medium. *Biology of Reproduction*, *99*(5), 938–948.

Degrelle, S. A., Blomberg, L. A., Garrett, W. M., Li, R. W., & Talbot, N. C. (2009). Comparative proteomic and regulatory network analyses of the elongating pig conceptus. *Proteomics*, *9*(10), 2678–2694.

D'Mello, J. P. F. (2003). Amino acids as multifunctional molecules, *Amino acids in animal nutrition* (2nd ed., pp. 1–14). Cambridge, MA: CABI Publishing.

Dienhart, M. K., O'Brien, M. J., & Downs, S. M. (1997). Uptake and salvage of hypoxanthine mediates developmental arrest in preimplantation mouse embryos. *Biology of Reproduction*, *56*(1), 1–13.

FASS. (2010). *Guide for care and use of agricultural animals in research and teaching* (3rd ed.). Champaign, IL: Federation of Animal Science Societies.

Forsey, K. E., Ellis, P. J., Sargent, C. A., Sturmey, R. G., & Leese, H. J. (2013). Expression and localization of creatine kinase in the preimplantation embryo. *Molecular Reproduction and Revelopment*, *80*(3), 185–192.

Fullerton, M. D., Hakimuddin, F., & Bakovic, M. (2007). Developmental and metabolic effects of disruption of the mouse CTP: Phosphoethanolamine cytidylyltransferase gene (Pcyt2). *Molecular and Cellular Biology*, *27*(9), 3327–3336.

Galea, E., Regunathan, S., Eliopoulos, V., & Feinstein, D. L. (1996). Inhibition of mammalian nitric oxide synthases by agmatine, an endogenous polyamine formed by decarboxylation of arginine. *Biochemical Journal*, *316*(1), 247–249.

Gardner, D. K. (1998). Changes in requirements and utilization of nutrients during mammalian preimplantation embryo development and their significance in embryo culture. *Theriogenology*, *49*(1), 83–102.

Garlow, J. E., Ka, H., Johnson, G. A., Burghardt, R. C., Jaeger, L. A., & Bazer, F. W. (2002). Analysis of osteopontin at the maternal-placental interface in pigs. *Biology of Reproduction*, *66*(3), 718–725.

Geisert, R. D., Brookbank, J. W., Michael Roberts, R., & Bazer, F. W. (1982). Establishment of pregnancy in the pig: II. Cellular remodeling of the porcine blastocyst during elongation on day 12 of pregnancy. *Biology of Reproduction*, *27*(4), 941–955.

Geisert, R. D., Ross, J. W., Ashworth, M. D., White, F. J., Johnson, G. A., & DeSilva, U. (2006). Maternal recognition of pregnancy signal or endocrine disruptor: The two faces of oestrogen during establishment of pregnancy in the pig. *Society of Reproduction and Fertility Supplement*, *62*, 131–145.

Gibson, K. M., Burlingame, T. G., Hogema, B., Jakobs, C., Schutgens, R. B. H., Millington, D., … Vockley, J. (2000). 2-Methylbutyryl-coenzyme A dehydrogenase deficiency: A new inborn error of L-isoleucine metabolism. *Pediatric Research*, *47*(6), 830–833.

Hammer, M. A., & Baltz, J. M. (2003). β-Alanine but not taurine can function as an organic osmolyte in preimplantation mouse embryos cultured from fertilized eggs. *Molecular Reproduction and Development: Incorporating Gamete Research*, *66*(2), 153–161.

Houghton, F. D., Thompson, J. G., Kennedy, C. J., & Leese, H. J. (1996). Oxygen consumption and energy metabolism of the early mouse

embryo. *Molecular Reproduction and Development: Incorporating Gamete Research*, *44*(4), 476–485.

Humpherson, P. G., Leese, H. J., & Sturmey, R. G. (2005). Amino acid metabolism of the porcine blastocyst. *Theriogenology*, *64*(8), 1852–1866.

Jaeger, C., Meret, M. l, Schmitt, C. A., & Lisec, J. (2017). Compound annotation in liquid chromatography/high-resolution mass spectrometry based metabolomics: Robust adduct ion determination as a prerequisite to structure prediction in electrospray ionization mass spectra. *Rapid Communications in Mass Spectrometry*, *31*(15), 1261–1266.

Kalhan, S. C., & Hanson, R. W. (2012). Resurgence of serine: An often neglected but indispensable amino Acid. *Journal of Biological Chemistry*, *287*(24), 19786–19791.

Karnovsky, A., Weymouth, T., Hull, T., Tarcea, V. G., Scardoni, G., Laudanna, C., … Omenn, G. S. (2012). Metscape 2 bioinformatics tool for the analysis and visualization of metabolomics and gene expression data. *Bioinformatics*, *28*(3), 373–380.

Kayser, J.-P. R., Kim, J. G., Cerny, R. L., & Vallet, J. L. (2006). Global characterization of porcine intrauterine proteins during early pregnancy. *Reproduction*, *131*(2), 379–388.

Khatchadourian, C., Guillaud, J., & Menezo, Y. (1994). Interactions in glycine and methionine uptake, conversion and incorporation into proteins in the preimplantation mouse embryo. *Zygote*, *2*(4), 301–306.

Kopka, J., Schauer, N., Krueger, S., Birkemeyer, C., Usadel, B., Bergmuller, E., … Steinhauser, D. (2004). GMD@ CSB. DB: The Golm metabolome database. *Bioinformatics*, *21*(8), 1635–1638.

Krisher, R. L., Heuberger, A. L., Paczkowski, M., Stevens, J., Pospisil, C., Prather, R. S., … Schoolcraft, W. B. (2015). Applying metabolomic analyses to the practice of embryology: Physiology, development and assisted reproductive technology. *Reproduction, Fertility, and Development*, *27*(4), 602–620.

Li, R., Whitworth, K., Lai, L., Wax, D., Spate, L., Murphy, C. N., … Prather, R. S. (2007). Concentration and composition of free amino acids and osmolalities of porcine oviductal and uterine fluid and their effects on development of porcine IVF embryos. *Molecular Reproduction and Development*, *74*(9), 1228–1235.

Lobo, M. V. T., Huerta, L., Arenas, M. I., Busto, R., Lasuncion, M. A., & Martin-Hidalgo, A. (2009). Hormone-sensitive lipase expression and IHC localization in the rat ovary, oviduct, and uterus. *Journal of Histochemistry & Cytochemistry*, *57*(1), 51–60.

Maiuolo, J., Oppedisano, F., Gratteri, S., Muscoli, C., & Mollace, V. (2016). Regulation of uric acid metabolism and excretion. *International Journal of Cardiology*, *213*, 8–14.

Mathew, D. J., Lucy, M. C., & Geisert, R. D. (2016). Interleukins, interferons, and establishment of pregnancy in pigs. *Reproduction*, *151*(6), R111–R122.

MATLAB. (2019). *version 9.6.0 (R2019a)*. Natick, MA: The MathWorks Inc.

Matsuo, S., Imai, E., Horio, M., Yasuda, Y., Tomita, K., Nitta, K., … Hishida, A. (2009). Revised equations for estimated GFR from serum creatinine in Japan. *American Journal of Kidney Diseases*, *53*(6), 982–992.

Meier, S., Trewhella, M. A., Fairclough, R. J., & Jenkin, G. (1997). Changes in uterine endometrial phospholipids and fatty acids throughout the oestrous cycle and early pregnancy in the ewe. *Prostaglandins, Leukotrienes and Essential Fatty Acids*, *57*(3), 341–349.

Miles, J. R., Freking, B. A., Blomberg, L. A., Vallet, J. L., & Zuelke, K. A. (2008). Conceptus development during blastocyst elongation in lines of pigs selected for increased uterine capacity or ovulation rate. *Journal of Animal Science*, *86*(9), 2126–2134.

Miles, J. R., Laughlin, T. D., Sargus-Patino, C. N., & Pannier, A. K. (2017). In vitro porcine blastocyst development in three-dimensional alginate hydrogels. *Molecular Reproduction and Development*, *84*(9), 775–787.

Moffett, J. R., & Namboodiri, M. A. (2003). Tryptophan and the immune response. *Immunology and Cell Biology*, *81*(4), 247–265.

Morgan, G. L., Geisert, R. D., Zavy, M. T., & Fazleabas, A. T. (1987). Development and survival of pig blastocysts after oestrogen administration on day 9 or days 9 and 10 of pregnancy. *Reproduction*, *80*(1), 133–141.

Murphy, S. P., Tayade, C., Ashkar, A. A., Hatta, K., Zhang, J., & Croy, B. A. (2009). Interferon gamma in successful pregnancies. *Biology of Reproduction*, *80*(5), 848–859.

Nelson, D. L., & Cox, M. M. (2013). Amino acid oxidation and the production of urea, *Lehninger principles of biochemistry* (6th ed., pp. 695–730). New York, NY: W. H. Freeman and Company.

Nochi, Z., Olsen, R. K. J., & Gregersen, N. (2017). Short-chain acyl-CoA dehydrogenase deficiency: From gene to cell pathology and possible disease mechanisms. *Journal of Inherited Metabolic Disease*, *40*(5), 641–655.

Patel, D., & Witt, S. N. (2017). Ethanolamine and phosphatidylethanolamine: Partners in health and disease. *Oxidative Medicine and Cellular Longevity*, *2017*.

Pope, W. F., & First, N. L. (1985). Factors affecting the survival of pig embryos. *Theriogenology*, *23*, 91–105.

Pope, W. F., Lawyer, M. S., Nara, B. S., & First, N. L. (1986). Effect of asynchronous superinduction on embryo survival and range of blastocyst development in swine. *Biology of Reproduction*, *35*(1), 133–137.

Pope, W. F., Maurer, R. R., & Stormshak, F. (1982). Survival of porcine embryos after asynchronous transfer. *Proceedings of the Society for Experimental Biology and Medicine*, *171*(2), 179–183.

R Core Team (2017). R: A language and environment for statistical computing. R Foundation for Statistical Computing, Vienna, Austria. Retrieved from https://www.R-project.org/

Richards, T., Wang, F., Liu, L., & Baltz, J. M. (2010). Rescue of postcompaction-stage mouse embryo development from hypertonicity by amino acid transporter substrates that may function as organic osmolytes. *Biology of Reproduction*, *82*(4), 769–777.

Saheki, T., Katsunuma, T., & Sase, M. (1977). Regulation of urea synthesis in rat liver: Changes of ornithine and acetylglutamate concentrations in the livers of rats subjected to dietary transitions. *The Journal of Biochemistry*, *82*(2), 551–558.

Salazar, J. H. (2014). Overview of urea and creatinine. *Laboratory Medicine*, *45*(1), e19–e20.

Samborski, A., Graf, A., Krebs, S., Kessler, B., & Bauersachs, S. (2013). Deep sequencing of the porcine endometrial transcriptome on day 14 of pregnancy. *Biology of Reproduction*, *88*(4), 84. 84, 81-13.

Shannon, P. (2003). Cytoscape: A software environment for integrated models of biomolecular interaction networks. *Genome Research*, *13*(11), 2498–2504.

Shuvalov, O., Petukhov, A., Daks, A., Fedorova, O., Vasileva, E., & Barlev, N. A. (2017). One-carbon metabolism and nucleotide biosynthesis as attractive targets for anticancer therapy. *Oncotarget*, *8*(14), 23955–23977.

Smith, C. A., Want, E. J., O'Maille, G., Abagyan, R., & Siuzdak, G. (2006). XCMS: Processing mass spectrometry data for metabolite profiling using nonlinear peak alignment, matching, and identification. *Analytical Chemistry*, *78*(3), 779–787.

Stacklies, W., Redestig, H., Scholz, M., Walther, D., & Selbig, J. (2007). pcaMethods—A bioconductor package providing PCA methods for incomplete data. *Bioinformatics*, *23*(9), 1164–1167.

Sturmey, R. G., Reis, A., Leese, H. J., & McEvoy, T. G. (2009). Role of fatty acids in energy provision during oocyte maturation and early embryo development. *Reproduction in Domestic Animals*, *44*, 50–58.

Sumner, L. W., Amberg, A., Barrett, D., Beale, M. H., Beger, R., Daykin, C. A., … Viant, M. R. (2007). Proposed minimum reporting standards for chemical analysis. *Metabolomics*, *3*(3), 211–221.

Tsugawa, H., Kind, T., Nakabayashi, R., Yukihira, D., Tanaka, W., Cajka, T., … Arita, M. (2016). Hydrogen rearrangement rules: Computational MS/MS fragmentation and structure elucidation using MS-FINDER software. *Analytical Chemistry*, *88*(16), 7946–7958.

Van Winkle, L. J., Haghighat, N., & Campione, A. L. (1990). Glycine protects preimplantation mouse conceptuses from a detrimental effect on development of the inorganic ions in oviductal fluid. *Journal of Experimental Zoology*, *253*(2), 215–219.

Waclawik, A. (2011). Novel insights into the mechanisms of pregnancy establishment: Regulation of prostaglandin synthesis and signaling in the pig. *Reproduction*, *142*(3), 389–399.

Wichers, M. C., & Maes, M. (2004). The role of indoleamine 2,3-dioxygenase (IDO) in the pathophysiology of interferon-alpha-induced depression. *Journal of Psychiatry and Neuroscience*, *29*(1), 11–17.

Wilde, M. H., Xie, S., Day, M. L., & Pope, W. F. (1988). Survival of small and large littermate blastocysts in swine after synchronous and asynchronous transfer procedures. *Theriogenology*, *30*(6), 1069–1074.

Yan, Y.-B. (2016). Creatine kinase in cell cycle regulation and cancer. *Amino Acids*, *48*(8), 1775–1784.

SUPPORTING INFORMATION

Additional supporting information may be found online in the Supporting Information section.

How to cite this article: Walsh SC, Miles JR, Yao L, et al. Metabolic compounds within the porcine uterine environment are unique to the type of conceptus present during the early stages of blastocyst elongation. *Mol Reprod Dev*. 2020;87: 174–190. https://doi.org/10.1002/mrd.23306